

## INVESTIGATION OF THE EFFECT OF SELECTED TRANSITION METAL SALTS ON THE PYROLYSIS OF HUADIAN OIL SHALE, CHINA

ZHIBING CHANG, MO CHU<sup>\*</sup>, CHAO ZHANG,  
SHUXIA BAI, HAO LIN, LIANGBO MA

School of Chemical and Environmental Engineering, China University of Mining and Technology (Beijing), Beijing 100083, P. R. China

**Abstract.** *In this paper, the effect of several transition metal salts such as  $\text{FeCl}_2 \cdot 4\text{H}_2\text{O}$ ,  $\text{CoCl}_2 \cdot 6\text{H}_2\text{O}$ ,  $\text{NiCl}_2 \cdot 6\text{H}_2\text{O}$  and  $\text{ZnCl}_2$  on oil shale pyrolysis was investigated, based on thermal decomposition characteristics and product yields and compositions. The salts were added individually to Chinese Huadian oil shale by physical mixing. Pyrolysis experiments of oil shale with and without transition metal salts were performed in a thermogravimetric analyzer and a fixed bed reactor. Thermogravimetric analysis (TGA) suggested that  $\text{CoCl}_2 \cdot 6\text{H}_2\text{O}$  and  $\text{NiCl}_2 \cdot 6\text{H}_2\text{O}$  could promote oil shale pyrolysis, leading to a greater thermogravimetric mass loss than raw oil shale. By contrast,  $\text{FeCl}_2 \cdot 4\text{H}_2\text{O}$  and  $\text{ZnCl}_2$  had only a slight effect on the decomposition behavior of oil shale. The results of fixed bed pyrolysis experiments showed that all metal salts enhanced the secondary cracking of shale oil, which decreased the oil yield and increased the pyrolytic gas yield. The metal salts could also catalyze the aromatization of aliphatic hydrocarbons to yield aromatic hydrocarbons. The catalytic activity of the studied salts decreased in the order  $\text{NiCl}_2 \cdot 6\text{H}_2\text{O} > \text{CoCl}_2 \cdot 6\text{H}_2\text{O} > \text{ZnCl}_2 > \text{FeCl}_2 \cdot 4\text{H}_2\text{O}$ .*

**Keywords:** *oil shale pyrolysis, transition metal salts, catalytic effect, shale oil cracking, aliphatic hydrocarbon aromatization.*

### 1. Introduction

The massive use of conventional fossil fuels causes their rapid depletion and increase in price. Therefore, it is especially significant nowadays to exploit unconventional alternative fossil fuels like oil shale (OS) [1]. Oil shale is a fine-grained sedimentary rock containing insoluble complex macromolecular organic matter called kerogen. Its vast reserves, which are widely spread all over the world, make oil shale one of the most promising alternative fossil

---

<sup>\*</sup> Corresponding author: e-mail [cm@cumb.edu.cn](mailto:cm@cumb.edu.cn)

fuels. Lately, the development and utilization of these energy resources has aroused significant interest worldwide [2].

Pyrolysis, also known as retorting, is one of the most attractive oil shale technologies. During the retorting process, the main organic matter in oil shale, kerogen, is converted into shale oil. To date, many operational parameters, including shale particle size [3], pyrolysis atmosphere [4], pyrolysis temperature [5] and heating rate [6], have been investigated in order to increase shale oil yield and improve its quality.

Several studies have also examined the effect of various catalysts on the pyrolysis of oil shale. Williams and Chishti [7, 8] investigated the effect of zeolite catalysts in a two-stage reactor. The researchers found that the use of these catalysts markedly decreased the content of nitrogen and sulfur in the produced shale oil. However, at the same time, the yield of shale oil was reduced. Gai et al. [9] studied the effect of pyrite on the pyrolysis of oil shale, showing that inherent pyrite could improve the oil yield; however, the additional pyrite promoted the evolution of volatiles. Hu et al. [10] noted that montmorillonite and gypsum could enhance the formation of oil and minimize the formation of residue during kerogen pyrolysis, while calcite inhibited oil formation. Using a dual-stage reactor, Lai et al. [11] demonstrated that oil shale ash had a catalytic effect on the secondary cracking and upgrading of shale oil to facilitate the conversion of the heavy oil fraction into light oil and gas.

The salts of transition metals such as Mn, Fe, Co, Ni, Cu and Zn are generally considered to catalyze coal pyrolysis. Iron-based catalysts, including  $\text{Fe}_2\text{O}_3$ , FeS and  $\text{FeSO}_4$ , have negative effects on the tar yield, favoring the formation of lighter species instead [12, 13].  $\text{CoCl}_2$  could promote the conversion of coal pyrolysis [14, 15]. In their work, Zou et al. [15] impregnated 15%  $\text{CoCl}_2$  to lignite, which increased the yield of total volatile matter more than two-fold in a spout-entrained reactor. Several authors [12, 14, 16] have noted that  $\text{ZnCl}_2$  leads to a higher coal conversion and a higher asphaltene yield. Considering the similarities between coal and oil shale, it is expected that transition metals might also play a catalytic role during oil shale degradation. Jiang et al. [17] investigated the catalytic effect of  $\text{CoCl}_2$  and  $\text{MnSO}_4$  on oil shale pyrolysis and the results showed that  $\text{CoCl}_2$  could act as the activation center to accelerate the breakdown of chemical bonds in organic matter, thereby increasing the yield of shale oil. However, only few studies examining the effect of different transition metals on the pyrolysis of oil shale have been reported to date.

In this study, pyrolysis experiments of Huadian oil shale in the absence and presence of transition metal salts ( $\text{FeCl}_2 \cdot 4\text{H}_2\text{O}$ ,  $\text{CoCl}_2 \cdot 6\text{H}_2\text{O}$ ,  $\text{NiCl}_2 \cdot 6\text{H}_2\text{O}$  and  $\text{ZnCl}_2$ ) were conducted in a thermogravimetric analyzer and a fixed bed pyrolyzer, in order to explore their potential catalytic effects on the process. The objective of this work was to provide the foundation for the design of potential catalysts for oil shale pyrolysis.

## 2. Experimental section

### 2.1. Materials

The oil shale used in this study was collected from Huadian city, Jilin province of China. The main characteristics of the oil shale sample are listed in Table 1. The sample was crushed and sieved to the size of 0–0.18 mm, and kept at room temperature for 48 h to give an air-dried sample, which was used for the pyrolysis experiments. In order to eliminate the effect of mineral components, the traditional HCl and HF washings were conducted to remove carbonates and silicates, respectively, resulting in the kerogen concentrate (Ker). In general, it was not possible to remove the inherent pyrite, FeS<sub>2</sub>, by using this method.

All transition metal salts (FeCl<sub>2</sub>·4H<sub>2</sub>O, CoCl<sub>2</sub>·6H<sub>2</sub>O, NiCl<sub>2</sub>·6H<sub>2</sub>O and ZnCl<sub>2</sub>) used in this work were of analytical grade. The salts were added to the oil shale or kerogen sample by physical mixing at 10 wt%. This amount was calculated using the ratio of the mass of pure metal salts (without crystallization water) to the dry and ash-free mass of oil shale or kerogen. The samples of oil shale and kerogen with added metal salts were denoted respectively OS-M and Ker-M, where M represents the type of metal element employed. For example, OS-Fe refers to the sample of oil shale mixed with FeCl<sub>2</sub>·4H<sub>2</sub>O, while Ker-Co designates the kerogen sample to which CoCl<sub>2</sub>·6H<sub>2</sub>O has been added.

**Table 1. Proximate, ultimate and Fischer assay analyses of Huadian oil shale**

Proximate analysis, wt%, ad		Ultimate analysis, wt%, ad		Fischer assay, wt%, ad	
Moisture	2.92	C	19.87	Shale oil	9.57
Volatile matter	25.03	H	2.84	Gas	3.50
Ash	70.45	N	4.82	Water	7.95
Fixed carbon	1.60	S	0.41	Residue	78.98

Note: ad – air-dried.

### 2.2. Thermogravimetric analysis

The thermogravimetric analysis (TGA) was carried out using a Mettler-Toledo TGA/DSC 1 thermogravimetric analyzer. Oil shale and kerogen samples were used in TGA. In each experiment, a sample weighing approximately 10 mg was distributed in a ceramic crucible. The sample was heated from ambient temperature to 550 °C at a heating rate of 10 °C/min, and then kept at 550 °C for 30 min. Nitrogen was used as the carrier gas (at 50 mL/min) in order to ensure an oxygen-free environment.

### 2.3. Fixed bed pyrolysis experiments

The schematic diagram of the fixed bed pyrolysis apparatus is shown in Figure 1. The pyrolyzer was constructed from aluminum according to the

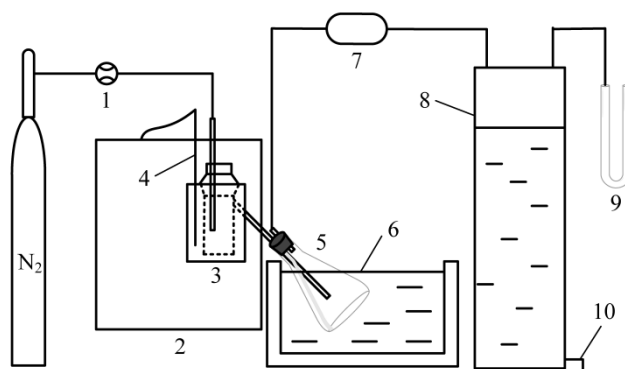


Fig. 1. Schematic diagram of the fixed bed pyrolysis apparatus. (1 – mass flow controller; 2 – electric-ring furnace; 3 – aluminum pyrolyzer; 4 – thermocouple; 5 – conical flask; 6 – ice-water bath; 7 – drying tube; 8 – acrylic glass cylinder; 9 – U-tube manometer; 10 – water faucet.)

national standard of China (SH/T 0508-92). In our work, a stainless steel pipe was attached to the cover of the retort for the carrier gas inlet. The raw oil shale and oil shale samples mixed with transition metal salts were employed in the pyrolysis experiments.

For each fixed bed pyrolysis experiment, approximately 50 g of the oil shale sample was placed inside the aluminum pyrolyzer. The pyrolyzer was installed in an electric-ring furnace with a thermocouple, and then heated from ambient temperature to 520 °C at 10 °C/min and held at 520 °C for 30 min. Nitrogen gas (50 mL/min) was introduced into the retort through the stainless steel pipe in order to sweep the volatile products towards the outlet of the retort. The resulting oil vapor, water steam and gases were directed into a conical flask, which was immersed in an ice-water bath. Most of the water and oil condensed in the conical flask, and the remaining fraction was captured using a drying tube filled with cotton wool and silica gel. The non-condensable gases were collected in an acrylic glass cylinder by using the water displacement method.

After the completion of each run, the apparatus was disassembled and the mass of shale char was weighed directly. The mass of the mixture of shale oil and water was determined from the mass difference of the collecting flask before and after the pyrolysis experiment. The mass of gases was calculated by material balance. The amount of water in the oil/water mixture was determined using the Dean-Stark extraction method. By this procedure, it was possible to obtain the mass of shale oil by subtracting the mass of the extracted water from the mass of the original mixture. The product yield was calculated by dividing the product mass by the mass of oil shale. Each pyrolysis experiment was performed in duplicate under identical conditions to assess the reproducibility of the test data. The final data listed below are the average values of the experimental results.

## 2.4. Analysis of shale oil and pyrolytic gas

The chemical composition of shale oil samples derived from raw oil shale or oil shale blended with transition metal salts was determined by gas chromatography-mass spectrometry (GC-MS) analysis, which was conducted on a Thermo SCIENTIFIC gas chromatograph equipped with a Trace 1300-ISQ mass spectrometer. The compounds present in shale oil were identified using the National Institute of Standards and Technology mass spectral library.

The non-condensable gases were sampled using gas sampling bags, and analyzed for their composition by using a BFTP SP2100A gas chromatograph (GC). The hydrocarbon gases ( $\text{CH}_4$ ,  $\text{C}_2\text{H}_6$ ,  $\text{C}_2\text{H}_4$ ,  $\text{C}_3\text{H}_8$ ,  $\text{C}_3\text{H}_6$ ,  $\text{C}_4\text{H}_{10}$  and  $\text{C}_4\text{H}_8$ ) were separated using a capillary column and identified by a flame ionization detector (FID). The non-hydrocarbon gases ( $\text{H}_2$ ,  $\text{CO}$  and  $\text{CO}_2$ ) were separated by two packed columns and identified using a thermal conductivity detector (TCD). The total gas volume and GC results were used to calculate the volume of each gas component.

## 3. Results and discussion

### 3.1. Thermogravimetric analysis

The thermogravimetric (TG) curves of oil shale and kerogen concentrate are shown in Figure 2a. For oil shale, the small mass loss below 200 °C is attributed to moisture evaporation, which includes the loss of the free water in the sample and the interlayer water from clay minerals. The mass loss in the temperature range of 200–350 °C was found to be negligible. However, once the temperature reached 350 °C, the decomposition of oil shale intensified dramatically up to 500 °C. The main mass loss occurring in this range is due to the pyrolysis of bitumen and kerogen present in the oil shale sample. The mass loss of the kerogen concentrate is significantly greater than that of raw oil shale. This outcome is expected as the organic matter was concentrated selectively with most of the mineral matter removed. In addition, a critical temperature of about 380 °C can be observed in the TG curve of kerogen. The rate of mass loss is low below 380 °C, which is due to the pyrolysis of kerogen to give pyrolytic bitumen and some gas products [18]. The rate of mass loss increases at temperatures above 380 °C, which can be attributed to the active cracking and vaporization of pyrolytic bitumen to yield shale oil, gases and char.

Figure 2b shows the TG curves of the employed pure transition metal salts.  $\text{FeCl}_2 \cdot 4\text{H}_2\text{O}$ ,  $\text{CoCl}_2 \cdot 6\text{H}_2\text{O}$  and  $\text{NiCl}_2 \cdot 6\text{H}_2\text{O}$  exhibit a marked mass loss below 160, 270 and 230 °C, respectively, stemming from the release of the crystallization water. After the initial mass loss, the rates of mass loss level off. There is almost no mass loss in the TG curve of  $\text{ZnCl}_2$  below 400 °C. However, the mass loss becomes significant above 400 °C as a result of the volatilization of  $\text{ZnCl}_2$ , as it has evidently low melting and boiling points, 290 and 733 °C, respectively.

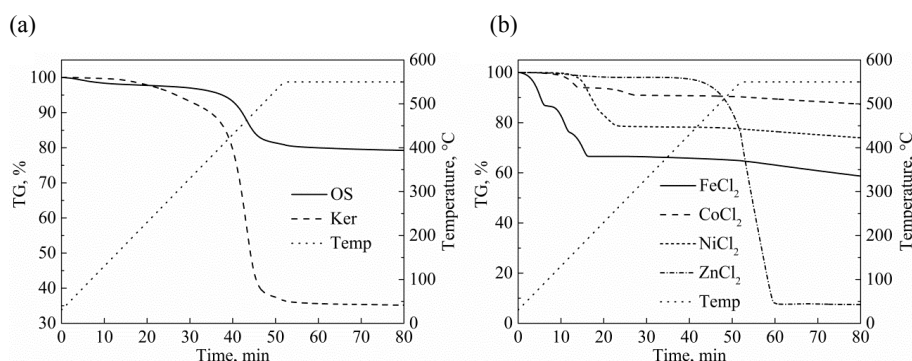


Fig. 2. TG curves of samples: (a) oil shale and kerogen; (b) pure transition metal salts.

The effect of transition metal salts on the pyrolysis of oil shale or kerogen was evaluated by comparing the TG curves obtained experimentally with the calculated TG curves. The calculated TG curves were obtained using the following equation:

$$W_{cal} = a \cdot W_{os-ker} + b \cdot W_{salt},$$

where  $W_{cal}$  is the calculated mass of the oil shale or kerogen sample mixed with transition metal salts at time  $t$ , %;  $W_{os-ker}$  is the mass of the individual oil shale or kerogen sample at time  $t$ , %;  $W_{salt}$  stands for the mass of the pure metal salt at time  $t$ , %;  $a$  denotes the initial mass percentage of oil shale or kerogen in the mixture;  $b$  signifies the initial mass percentage of metal salts in the mixture where  $a + b = 1$ . A negative difference between the experimental and calculated TG curves, i.e. when the mass loss determined experimentally is greater than the calculated mass loss, may indicate that the metal salts have a catalytic effect on the conversion of oil shale or kerogen.

Figure 3 compares the experimental and calculated TG curves for the oil shale and kerogen samples mixed with transition metal salts. For the oil shale sample blended with  $\text{FeCl}_2 \cdot 4\text{H}_2\text{O}$ , the experimental mass loss is greater than the calculated one at temperatures above 300 °C (Fig. 3a). However, the addition of this Fe salt caused a decrease in the mass loss of kerogen in the temperature range of 30–380 °C and at the isothermal stage (50–80 min), which may indicate an inhibitive effect of  $\text{FeCl}_2 \cdot 4\text{H}_2\text{O}$  on the kerogen degradation. The increased mass loss in oil shale may be attributed to the interaction between minerals present in oil shale and  $\text{FeCl}_2 \cdot 4\text{H}_2\text{O}$ .

Figure 3b shows that for both oil shale and kerogen, the addition of  $\text{CoCl}_2 \cdot 6\text{H}_2\text{O}$  increases the sample mass loss over the entire time period of the experiment. The experimental values of the final mass loss for oil shale and kerogen are 23.4 and 63.0 wt%, respectively, which are higher by 2.8 and 2.4 wt% compared to the calculated values of oil shale and kerogen.

Therefore, these results indicate that  $\text{CoCl}_2 \cdot 6\text{H}_2\text{O}$  may catalyze the pyrolysis of kerogen and increase its conversion to shale oil.

For oil shale and kerogen samples mixed with  $\text{NiCl}_2 \cdot 6\text{H}_2\text{O}$ , the experimental mass loss exceeded the calculated one at temperatures above 260 °C (Fig. 3c). However, the difference in mass loss is rather small. The experimental TG curve of kerogen almost overlaps with the calculated one at the isothermal stage. These results suggest that  $\text{NiCl}_2 \cdot 6\text{H}_2\text{O}$  might exert a slight catalytic effect on the pyrolysis process.

Figure 3d shows that  $\text{ZnCl}_2$  increases the mass loss of oil shale and kerogen below 450 °C, which indicates that this compound may catalyze kerogen pyrolysis at low temperatures. At temperatures above 450 °C, the experimental mass loss of oil shale and especially kerogen is clearly lower than their calculated mass loss. Since  $\text{ZnCl}_2$  starts to volatilize rapidly at 450 °C, the kerogen- $\text{ZnCl}_2$  interaction may resist the volatilization of  $\text{ZnCl}_2$ .

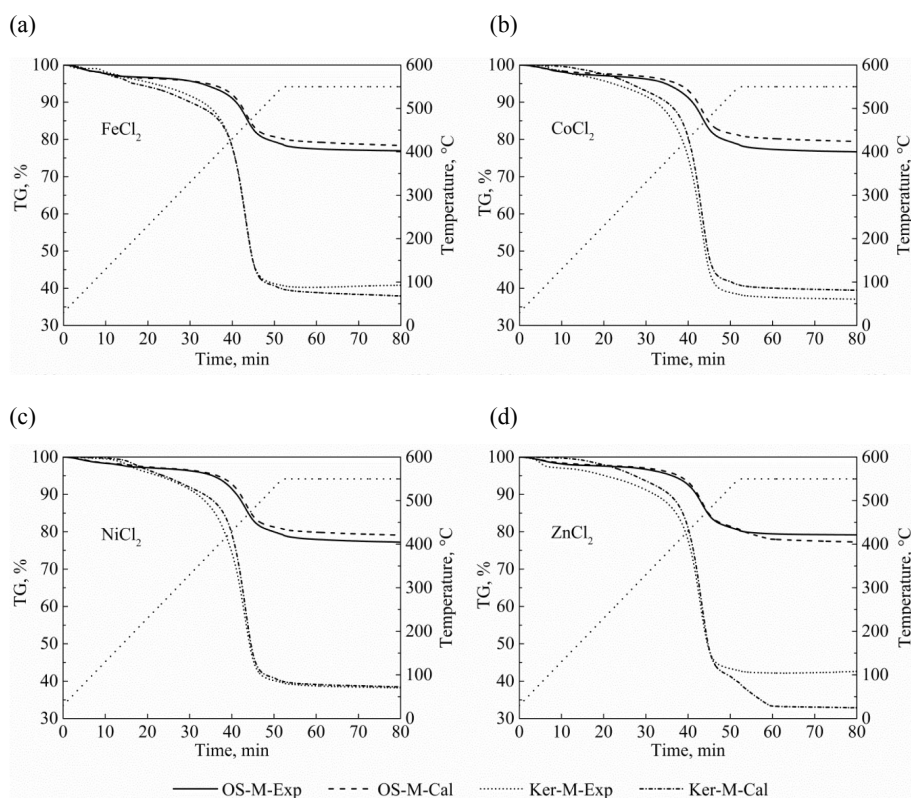


Fig. 3. Experimental and calculated TG curves for oil shale and kerogen samples mixed with transition metal salts: (a)  $\text{FeCl}_2$ ; (b)  $\text{CoCl}_2$ ; (c)  $\text{NiCl}_2$ ; (d)  $\text{ZnCl}_2$ .

### 3.2. Product yields in fixed bed pyrolysis experiments

The yields of pyrolytic products of Huadian oil shale mixed with transition metal salts are summarized in Figure 4. The shale char yield decreased upon addition of  $\text{FeCl}_2 \cdot 4\text{H}_2\text{O}$ ,  $\text{CoCl}_2 \cdot 6\text{H}_2\text{O}$  and  $\text{NiCl}_2 \cdot 6\text{H}_2\text{O}$ . These trends are more or less in accord with the results of the thermogravimetric analysis, as these three transition metal salts increase the mass loss of oil shale by pyrolysis.

Unfortunately, the shale oil yield decreases while the gas yield increases in the presence of transition metal salts. These results are inconsistent with the findings of Jiang et al. [17] who noticed that  $\text{CoCl}_2 \cdot 6\text{H}_2\text{O}$  could promote shale oil formation and resist pyrolytic gas evolution. The main reason for this discrepancy can be attributed to the different particle sizes of oil shale samples. A previous work employed oil shale samples with a large particle size, 6–15 mm, whereas the current study utilized the 0–0.18 mm particle size of oil shale to facilitate TG experiments. The packing of large oil shale particles in a fixed bed reactor leads to a rather great void volume, through which the oil vapor can move from the reactor easily. However, small particles pack more efficiently, causing a significant reduction in the void volume, thereby increasing the residence time of the oil vapor in the packed bed. Most importantly, for oil shale mixed with transition metal salts, the activation centers may exert a catalytic cracking effect on the oil components as they move through the compact particle bed, which decreases the quantity of shale oil and increases that of the gaseous products. The other possible reason for this discrepancy may be the use of a different method to add the salts. The solution impregnation method used in the previous study may lead to a more even distribution of transition metal salts in the sample than the physical mixing employed in this work. The catalytic effect of transition metals may be maximized in the former case.

Figure 4 also shows that the water yield increases in OS-Fe, OS-Co and OS-Ni samples. This observation is not surprising since these salts contain a certain amount of crystallization water, which is released during thermal heating.

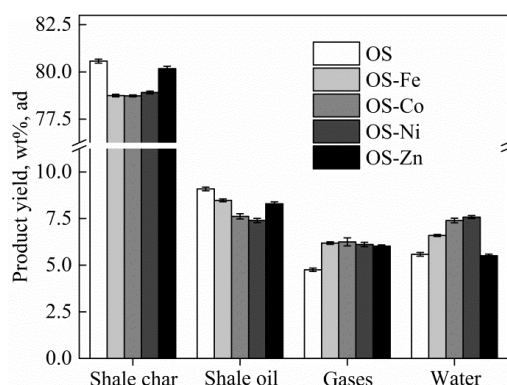


Fig. 4. The effect of transition metal salts on the product yield of oil shale pyrolysis.

### 3.3. Shale oil characterization

Figure 5 compares the GC-MS spectra of shale oils resulting from oil shale mixed with different transition metal salts. All chromatograms are

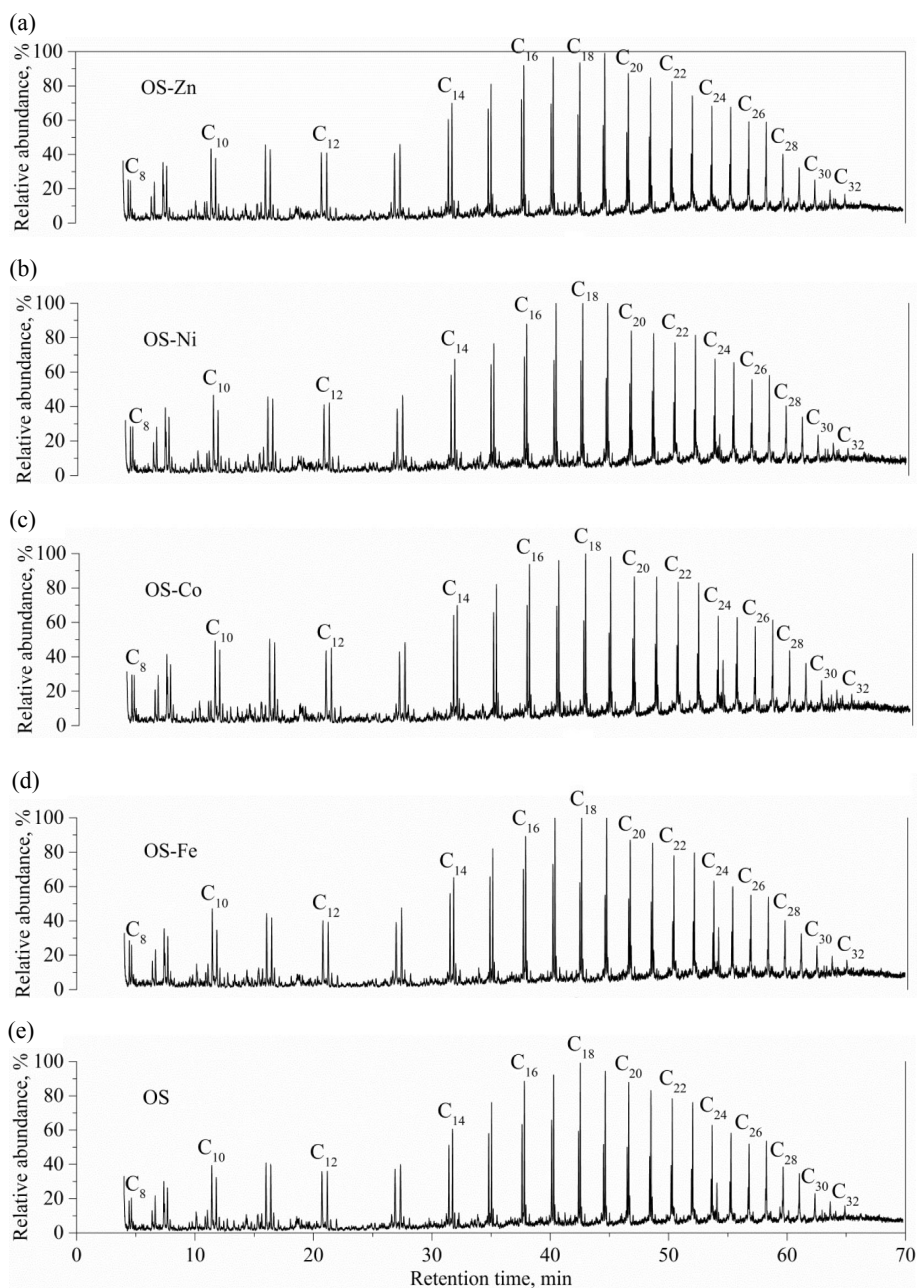


Fig. 5. Comparison of total ion chromatograms of shale oil samples mixed with salts of transition metals: (a) Zn; (b) Ni; (c) Co; (d) Fe; (e) unmixed OS sample.

dominated by alkanes and alkenes with 8–32 carbon atoms, and the peak from each *n*-alkane is accompanied by a peak from the corresponding *n*-alkene. Aromatic hydrocarbons and oxygenated compounds, e.g., acids, alcohols, esters, ketones and phenols, were also identified during the GC-MS analyses. These results are in good agreement with the results reported previously by other researchers [19].

In order to estimate the effect of transition metal salts on the shale oil composition, the ion peak area is used to give the relative content of the main classes of components, as shown in Table 2. It demonstrates that the addition of transition metal salts decreases the alkane content and increases both the alkene content and the alkenes/alkanes ratio. In his study, Ballice [20] used the alkenes/alkanes ratio to evaluate the cracking reactions of aliphatic hydrocarbons. The cracking reactions have been shown to proceed via a free radical mechanism to give smaller linear alkanes and alkenes, therefore increasing the alkenes/alkanes ratio. Thus, the transition metal salts in this study seem to catalyze the cracking of aliphatic hydrocarbons. Furthermore, the variation in OS-Co and OS-Ni samples is more pronounced than that in OS-Fe and OS-Zn samples, which is indicative of a strong catalytic effect exerted by  $\text{CoCl}_2 \cdot 6\text{H}_2\text{O}$  and  $\text{NiCl}_2 \cdot 6\text{H}_2\text{O}$ .

Additionally, the content of aromatic hydrocarbons is subject to the following order: OS-Ni > OS-Co > OS-Zn > OS-Fe > OS, suggesting that the metal salts may catalyze the aromatization of aliphatic hydrocarbons and  $\text{CoCl}_2 \cdot 6\text{H}_2\text{O}$  and  $\text{NiCl}_2 \cdot 6\text{H}_2\text{O}$  exhibit the highest catalytic activity. These results may be related to the strong Lewis acidity of the Co and Ni salts, as verified by Han et al. [21]. The formation of aromatic hydrocarbons was proposed to involve the following conversions: cracking of large aliphatic hydrocarbons to yield low-molecular-weight (LMW) alkanes and alkenes, which is catalyzed by the strongly acidic sites in  $\text{CoCl}_2 \cdot 6\text{H}_2\text{O}$  and  $\text{NiCl}_2 \cdot 6\text{H}_2\text{O}$ , cyclization of LMW alkenes and dialkenes to form cyclic alkenes, and dehydrogenation of cyclic alkenes to yield aromatic hydrocarbons [22]. From Table 2 it can also be seen that the quantity of oxygen-containing compounds increases in the presence of transition metal salts. The reason for this tendency is not completely clear at this stage.

**Table 2. The relative content of major components in shale oils derived from oil shales mixed with transition metal salts**

Compound	Content, area%				
	OS	OS-Fe	OS-Co	OS-Ni	OS-Zn
Alkanes	55.84	53.02	50.07	48.03	53.30
Alkenes	35.79	37.15	37.12	36.87	36.29
Aromatic hydrocarbons	4.87	5.12	7.53	9.18	5.84
Oxygenated compounds	3.5	4.71	5.29	5.92	4.57
Alkenes/alkanes	0.64	0.70	0.74	0.77	0.68

The *n*-alkanes and *n*-alkenes in shale oil samples can be divided, according to number of carbon atoms, into the following groups: C<sub>8</sub>–C<sub>16</sub>, C<sub>17</sub>–C<sub>24</sub> and C<sub>25</sub>–C<sub>32</sub>. The contents of these groups based on the peak areas are normalized to 100% (Fig. 6). Although not very obvious, it is possible to observe that the presence of transition metal salts results in a decrease in the content of long-chain aliphatic hydrocarbons and an increase in the short-chain hydrocarbons. This result provides a direct evidence for the catalytic effect of metal salts on the cracking of aliphatic hydrocarbons. Furthermore, the greater variation in aliphatic hydrocarbons content in OS-Co and OS-Ni samples is indicative of a strong catalytic activity of CoCl<sub>2</sub>·6H<sub>2</sub>O and NiCl<sub>2</sub>·6H<sub>2</sub>O.

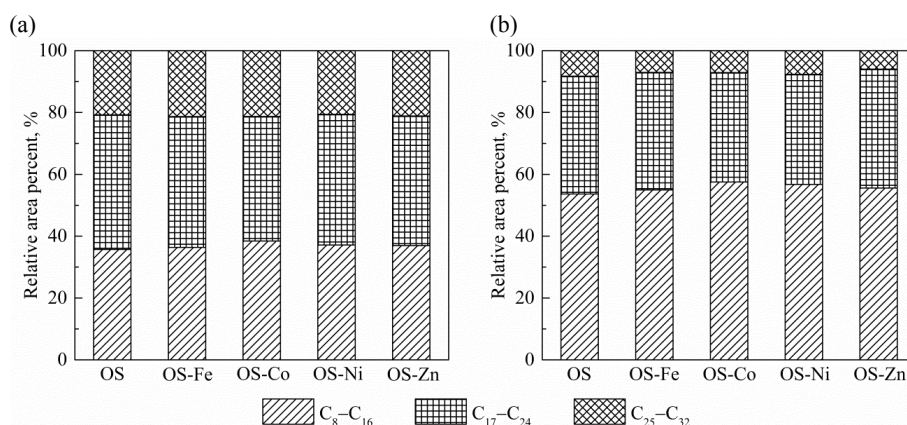


Fig. 6. Carbon number distribution of aliphatic hydrocarbons present in shale oils: (a) *n*-alkanes; (b) *n*-alkenes.

### 3.4. Pyrolytic gas characterization

Table 3 presents the yields of non-hydrocarbon gases in oil shale samples mixed with different transition metal salts. It is revealed that the salts have a different effect on the gases yields. The hydrogen yield decreases in the order OS-Ni > OS-Co > OS-Zn > OS-Fe > OS, which is in accord with the variation in the content of aromatic hydrocarbons (Table 2). Thus, the extra hydrogen determined for the samples mixed with the metal salts is derived primarily from the aromatization of aliphatic hydrocarbons. The addition of transition metal salts also led to a notable increase in the yield of carbon dioxide. According to Han et al. [21], the chlorides of Co and Ni can be reduced by coal char during pyrolysis to release chloride anion. Considering the similarity between coal and oil shale, the chlorides in this study could be also reduced by the organic carbon of oil shale. The released chloride anion would be expected to firstly form HCl, which could react further with the carbonate minerals of oil shale to generate carbon dioxide. While the yield of

**Table 3. Yields of non-hydrocarbon gases in oil shale samples mixed with transition metal salts**

Non-hydrocarbon gas	Gas yield, mL/g				
	OS	OS-Fe	OS-Co	OS-Ni	OS-Zn
Hydrogen	6.70	8.30	13.90	14.33	11.21
Carbon dioxide	11.31	18.62	17.98	17.35	17.58
Carbon monoxide	0.02	0.07	0.09	0.04	0.05

carbon monoxide is rather low in comparison to the yield of carbon dioxide, it also increases in the presence of metal salts.

Table 4 gives the yields of hydrocarbon gases in oil shale samples mixed with different transition metal salts. It is clear from the table that the salts exert a different effect on these yields. The presence of Fe chloride increases the yield of all hydrocarbon gases except methane. In contrast, the Co, Ni, and Zn chlorides decrease the yields of methane, ethane, ethene and propane, and increase those of propene, butane and butene, which may be related to the aromatization of aliphatic hydrocarbons. The alkenes to alkanes ratio in pyrolytic gases has been used to study the reaction mechanisms and reflects the pyrolysis conditions [5, 22]. For example, Wang et al. [5] suggested that the increase in the alkenes/alkanes ratio with increasing pyrolysis temperature is related to the intensification of the secondary gas phase cracking reactions. It is clear from Table 4 that addition of transition metal salts results in an increase in ethene/ethane, propene/propane and butene/butane ratios. The total alkenes/alkanes gas ratio also increases slightly from 0.26 to 0.29 following the addition of transition metal salts. The increased alkene/alkane ratios can be attributed to the catalytic effect of these metal salt additives on the cracking reaction of shale oil.

**Table 4. Yields of hydrocarbon gases in oil shale samples mixed with transition metal salts**

Hydrocarbon gas	Gas yield, mL/g				
	OS	OS-Fe	OS-Co	OS-Ni	OS-Zn
Methane	4.01	3.96	3.81	3.81	3.87
Ethane	1.65	1.67	1.51	1.50	1.56
Propane	0.65	0.67	0.60	0.62	0.62
Butane	0.25	0.30	0.28	0.28	0.28
Ethene	0.71	0.73	0.68	0.68	0.67
Propene	0.81	0.94	0.86	0.85	0.85
Butene	0.16	0.23	0.25	0.25	0.23
Total alkanes	6.56	6.60	6.20	6.21	6.32
Total alkenes	1.68	1.89	1.79	1.77	1.74
Total hydrocarbons	8.24	8.49	7.99	7.98	8.06
Ethene/ethane	0.43	0.44	0.45	0.45	0.43
Propene/propane	1.25	1.39	1.44	1.38	1.37
Butene/butane	0.63	0.76	0.88	0.88	0.82
Alkenes/alkanes	0.26	0.29	0.29	0.29	0.28

#### 4. Conclusions

In this study, the effect of transition metal salts  $\text{FeCl}_2 \cdot 4\text{H}_2\text{O}$ ,  $\text{CoCl}_2 \cdot 6\text{H}_2\text{O}$ ,  $\text{NiCl}_2 \cdot 6\text{H}_2\text{O}$  and  $\text{ZnCl}_2$  on the pyrolysis of Huadian oil shale was investigated. The oil shale pyrolysis experiments were conducted in the absence and presence of metal salts first in a thermal gravimetric analyzer to study the thermal decomposition characteristics. Next, oil shale pyrolysis was performed in a fixed bed reactor to examine the yield and composition of the pyrolytic products. The following conclusions can be drawn from the experimental results:

1. The pyrolysis behavior analysis indicated that  $\text{CoCl}_2 \cdot 6\text{H}_2\text{O}$  and  $\text{NiCl}_2 \cdot 6\text{H}_2\text{O}$  exerted a catalytic effect on the oil shale pyrolysis, producing a greater thermogravimetric mass loss in comparison to raw oil shale. By contrast,  $\text{FeCl}_2 \cdot 4\text{H}_2\text{O}$  and  $\text{ZnCl}_2$  were found to have only a slight effect on the thermal decomposition of oil shale.
2. In the fixed bed pyrolysis reactor, the transition metal salts were all observed to catalyze the secondary cracking reaction of shale oil, which led to a lower oil yield and a higher gas yield when compared to the original oil shale. In addition, the characterization of shale oil and non-condensable gases showed that these additives could catalyze the cracking and aromatization of aliphatic hydrocarbons, and the catalytic effect was subject to the following order:  $\text{NiCl}_2 \cdot 6\text{H}_2\text{O} > \text{CoCl}_2 \cdot 6\text{H}_2\text{O} > \text{ZnCl}_2 > \text{FeCl}_2 \cdot 4\text{H}_2\text{O}$ .

#### Acknowledgements

The study was financially supported by the National Basic Research Program of China (Grant No. 2014CB744301).

#### REFERENCES

1. Siirde, A. Oil shale – global solution or part of the problem. *Oil Shale*, 2008, **25**(2), 201–202.
2. Altun, N. E., Hiçyilmaz, C., Hwang, J.-Y., Suat Bağcı, A., Kök, M. V. Oil shales in the world and Turkey; reserves, current situation and future prospects: a review. *Oil Shale*, 2006, **23**(3), 211–227.
3. Nazzal, J. M. The influence of grain size on the products yield and shale oil composition from the pyrolysis of Sultani oil shale. *Energ. Convers. Manage.*, 2008, **49**(11), 3278–3286.
4. Xie, F. F., Wang, Z., Lin, W. G., Song, W. L. Study on thermal conversion of Huadian oil shale under  $\text{N}_2$  and  $\text{CO}_2$  atmospheres. *Oil Shale*, 2010, **27**(4), 309–320.
5. Wang, S., Jiang, X. M., Han, X. X., Tong, J. H. Effect of retorting temperature on product yield and characteristics of non-condensable gases and shale oil obtained by retorting Huadian oil shales. *Fuel Process. Technol.*, 2014, **121**, 9–15.

6. Wang, S., Liu, J. X., Jiang, X. M., Han, X. X., Tong, J. H. Effect of heating rate on products yield and characteristics of non-condensable gases and shale oil obtained by retorting Dachengzi oil shale. *Oil Shale*, 2013, **30**(1), 27–47.
7. Williams, P. T., Chishti, H. M. Two stage pyrolysis of oil shale using a zeolite catalyst. *J. Anal. Appl. Pyrol.*, 2000, **55**(2), 217–234.
8. Williams, P. T., Chishti, H. M. Influence of residence time and catalyst regeneration on the pyrolysis–zeolite catalysis of oil shale. *J. Anal. Appl. Pyrol.*, 2001, **60**(2), 187–203.
9. Gai, R. H., Jin, L. J., Zhang, J. B., Wang, J. Y., Hu, H. Q. Effect of inherent and additional pyrite on the pyrolysis behavior of oil shale. *J. Anal. Appl. Pyrol.*, 2014, **105**, 342–347.
10. Hu, M. J., Cheng, Z. Q., Zhang, M. Y., Liu, M. Z., Song, L. H., Zhang, Y. Q., Li, J. F. Effect of calcite, kaolinite, gypsum, and montmorillonite on Huadian oil shale kerogen pyrolysis. *Energ. Fuel.*, 2014, **28**(3), 1860–1867.
11. Lai, D. G., Chen, Z. H., Lin, L. X., Zhang, Y. M., Gao, S. Q., Xu, G. W. Secondary cracking and upgrading of shale oil from pyrolyzing oil shale over shale ash. *Energ. Fuel.*, 2015, **29**(4), 2219–2226.
12. Pinto, F., Gulyurtlu, I., Lobo, L. S., Cabrita, I. The effect of catalysts blending on coal hydrolysis. *Fuel*, 1999, **78**(7), 761–768.
13. Feng, J., Xue, X. Y., Li, X. H., Li, W. Y., Guo, X. F., Liu, K. Products analysis of Shendong long-flame coal hydrolysis with iron-based catalysts. *Fuel Process. Technol.*, 2015, **130**, 96–100.
14. Öztaş, N. A., Yürüm, Y. Effect of catalysts on the pyrolysis of Turkish Zonguldak bituminous coal. *Energ. Fuel.*, 2000, **14**(4), 820–827.
15. Zou, X. W., Yao, J. Z., Yang, X. M., Song, W. L., Lin, W. G. Catalytic effects of metal chlorides on the pyrolysis of lignite. *Energ. Fuel.*, 2007, **21**(2), 619–624.
16. Kandiyoti, R., Lazaridis, J. I., Dyrvold, B., Weerasinghe, C. R. Pyrolysis of a ZnCl<sub>2</sub>-impregnated coal in an inert atmosphere. *Fuel*, 1984, **63**(11), 1583–1587.
17. Jiang, H. F., Song, L. H., Cheng, Z. Q., Chen, J., Zhang, L., Zhang, M. Y., Hu, M. J., Li, J. N., Li, J. F. Influence of pyrolysis condition and transition metal salt on the product yield and characterization via Huadian oil shale pyrolysis. *J. Anal. Appl. Pyrol.*, 2015, **112**, 230–236.
18. Li, Q. Y., Han, X. X., Liu, Q. Q., Jiang, X. M. Thermal decomposition of Huadian oil shale. Part 1. Critical organic intermediates. *Fuel*, 2014, **121**, 109–116.
19. Lin, L. X., Zhang, C., Li, H. J., Lai, D. G., Xu, G. W. Pyrolysis in indirectly heated fixed bed with internals: The first application to oil shale. *Fuel Process. Technol.*, 2015, **138**, 147–155.
20. Ballice, L. Effect of demineralization on yield and composition of the volatile products evolved from temperature-programmed pyrolysis of Beypazari (Turkey) oil shale. *Fuel Process. Technol.*, 2005, **86**(6), 673–690.
21. Han, J. Z., Wang, X. D., Yue, J. R., Gao, S. Q., Xu, G. W. Catalytic upgrading of coal pyrolysis tar over char-based catalysts. *Fuel Process. Technol.*, 2014, **122**, 98–106.
22. Nazzal, J. M. Influence of heating rate on the pyrolysis of Jordan oil shale. *J. Anal. Appl. Pyrol.*, 2002, **62**, 225–238.

Presented by X. Han

Received October 1, 2016